ISSN 2096-7071
CN 10-1629/R1

CHINA CDC WEEKLY

Vol. 3 No. 20 May 14, 2021

CCDC weekly

中国疾病预防控制中心周报

ISSN 2096-7071

Cover Photo: China CDC's campus in Changping District, Beijing. Photographer: Huanyong Du, China Academy of Safety Science and Technology.

Methods and Applications

Trend Analysis and Intervention Effect Starting Point Detection of COVID-19 Epidemics Using Recalibrated Time Series Models — Worldwide, 2020

Shu Li[1,&]; Chen Chen[2,&]; Shuyin Cao[1]; Kejia Hu[1]; Hao Lei[1]; Xiaolin Xu[1]; Qinchuan Wang[3]; Changzheng Yuan[1]; Sicong Wang[1]; Sisi Wang[1]; Junlin Jia[1]; Yuanqing Ye[1,2]; Xifeng Wu[1,2,#]

ABSTRACT

Objective: This study aimed to identify a model for short-term coronavirus disease 2019 (COVID-19) trend prediction and intervention evaluation.

Methods: We compared the autoregressive integrated moving average (ARIMA) model and Holt exponential smoothing (Holt) model on predicting the number of cumulative COVID-19 cases in China. Based on the mean absolute percentage error (MAPE) value, the optimal model was selected and further tested using data from the United States, Italy and Republic of Korea. The intervention effect starting time points and abnormal trend changes were detected by observing the pattern of differences between the predicted and real trends.

Results: The recalibrated ARIMA model with a 5-day prediction time span has the best model performance with MAPEs ranged between 2% and 5%. The intervention effects started to show on February 7 in the mainland of China, March 5 in Republic of Korea and April 27 in Italy, but have not been detected in the US as of May 19. Temporary abnormal trends were detected in Korea and Italy, but the overall epidemic trends were stable since the effect starting points.

Conclusion: The recalibrated ARIMA model can detect the intervention effects starting points and abnormal trend changes; thus to provide valuable information support for epidemic trend analysis and intervention evaluation.

INTRODUCTION

Coronavirus disease 2019 (COVID-19) is still a worldwide threat (*1*). Previous studies have developed a variety of mathematical models to simulate and predict the disease transmission pattern recently (*2*–*3*), which mainly focus on macro-level and long-term prediction over the entire course of an pandemic. However, those models may miss real-time trend changes and shorter-time disturbances. In this study, a model for short-term trend predictions and evaluation of interventions was developed. By comparing the autoregressive integrated moving average (ARIMA) model and Holt exponential smoothing (Holt) model on effects of predicting the number of cumulative cases in different regions and countries, the optimal model was identified and further tested using data from the US, Italy, and Republic of Korea. The results indicated that the recalibrated ARIMA model was suitable for short-term prediction of COVID-19 trends and could detect the intervention effect starting time points. Based on the analysis, the effects of interventions started to show on February 7, 2020 in the mainland of China, March 5, 2020 in Republic of Korea, April 27, 2020 in Italy, and May 19, 2020 in the United States. This model can provide valuable information to support evaluating interventions, resource allocation, decision-making, and situation monitoring. Given the ongoing COVID-19 pandemic, this study could serve as a reference to initiate more adaptable and practice-based epidemic trend analysis tools that can benefit pandemic responders in different countries.

METHODS

Data of confirmed cases in the mainland of China were obtained from the official websites of China's National Health Commission and local health commissions. Hubei Province was excluded since its diagnostic criteria was revised (*4*). The numbers of cumulative confirmed cases in Guangdong, Henan, Zhejiang, Hunan, and Anhui provinces, as well as the total number of cases in the mainland of China (except Hubei), were used for developing the model. Provincial data from the report starting date to February 24, 2020, and national data from January 19 to February

24, 2020 were included for analysis. The daily cumulative number of confirmed cases in the US, Republic of Korea, and Italy were collected from the World Health Organization (WHO) COVID-19 situation reports and the Johns Hopkins University dashboard (*5*), and these data were used for model testing and trend analysis.

ARIMA and Holt models were applied for short-term prediction on daily number of cumulative cases in China (except Hubei) and selected provinces. The ARIMA model capitalized on the associations in the sequentially lagged relationships that exist in the given dataset. The Holt method, also known as the double exponential model, is an extension of single exponential smoothing and can be used to analyze the time series data with levels and trends. Model performance was compared across a 5-day, a 6-day, and a 7-day prediction time spans, respectively. Mean absolute percentage error (MAPE) (Equation 1) was used to evaluate the prediction accuracy between the predicted and actual values, and the model with the best MAPE was selected.

$$MAPE = \frac{\sum \frac{|A-P|}{A} \times 100}{N} \quad (1)$$

A: actual value; *P*: predicted value; *N*: number of days predicted.

The mainland of China (except Hubei) with a 5-day prediction time span was used as an example. First, the number of daily cumulative cases from the first day to January 31, 2020 was used for prediction from February 1 to February 5. Then, data as of February 5 were used for prediction from February 6 to February 10, and the prediction would loop to the next 5-day span until February 24. The prediction was made for every 5-day period and each model was re-calibrated by including updated data. The epidemic trend was analyzed by applying the optimal model on data of the US, Italy, and Republic of Korea. Predictions started when the new cases were reported for three consecutive days. Therefore, the confirmed cases of the US, Republic of Korea, and Italy since the first report day to March 20, February 18, and February 23 was used as the first training set. Subsequent predictions were done every 5 days until May 19, 2020 using the same method. Since the prediction error tends to increase as the prediction time extend, only the predicted values for every fifth day were kept to exclude the influence of prediction error on epidemic trend analysis. By analyzing the pattern of differences between predicted and observed trends (Equation 2), the time points that might reflect either the starting of intervention effect or the occurrence of unexpected incidents can be detected. For example, if a negative difference pattern (more actual cases than predicted) changed to a positive one (more predicted cases than actual), the changing point might reflect the effects of interventions since the predicted trend still followed the previous upward trend pattern, whereas the real trend was flattened due to intervention effects.

$$Difference = P - A \quad (2)$$

Modelling analysis were performed using *auto.arima()* and *holt()* functions in the forecast

TABLE 1. MAPEs between reported and predicted numbers of COVID-19 cases of the mainland of China (excluding Hubei Province) and five provinces in China using ARIMA and Holt models (%).

Area	Models	MAPEs					
		February 1–5	February 6–10	February 11–15	February 16–20	February 21–24	February 1–24
The mainland of China	ARIMA	0.99	4.14	1.28	1.07	6.25	2.60
	Holt	0.87	4.15	1.86	1.69	4.61	2.55
Guangdong	ARIMA	14.80	5.01	0.89	3.13	0.54	5.05
	Holt	14.80	4.95	1.21	4.76	0.63	5.47
Zhejiang	ARIMA	2.99	5.16	1.99	0.57	5.64	3.17
	Holt	3.82	5.16	3.45	0.64	5.64	3.66
Henan	ARIMA	4.94	8.58	0.40	1.71	0.14	3.28
	Holt	4.94	8.63	1.22	2.41	0.14	3.61
Hunan	ARIMA	4.91	2.84	1.62	0.32	0.17	2.05
	Holt	13.60	4.11	3.53	0.87	0.10	4.62
Anhui	ARIMA	2.03	2.02	2.21	4.36	0.20	2.25
	Holt	14.27	2.10	4.64	1.85	0.05	4.77

Abbreviations: ARIMA=autoregressive integrated moving average model; COVID-19=coronavirus disease 2019; Holt=Holt exponential smoothing model; MAPEs=mean absolute percentage errors.

package in *R* software (version 3.6.2; RStudio Inc; US) (*6*).

RESULTS

For a 5-day prediction time span, both ARIMA and Holt models showed excellent model performance (MAPE <5%) regardless of study regions (Table 1). The overall prediction accuracy of the ARIMA model was slightly better (overall MAPEs: 3.07% *vs.* 4.11%) than the Holt model (Figure 1). Lower MAPEs were observed in 5-day prediction (3.07%, range: 2.05%–5.05%) compared to that in the 6-day (4.31%, range: 3.06%–6.72%), and the 7-day (5.13%, range: 2.02%–10.26%) predictions. The Holt model yielded the similar result and also favored the 5-day prediction span.

Based on the results, the ARIMA model with a 5-day prediction time span was further tested using data from the US, Italy, and Republic of Korea. ARIMA also performed well for the other three countries in the late-stages (Figure 2). Almost all the difference values were positive after February 7 in the mainland of

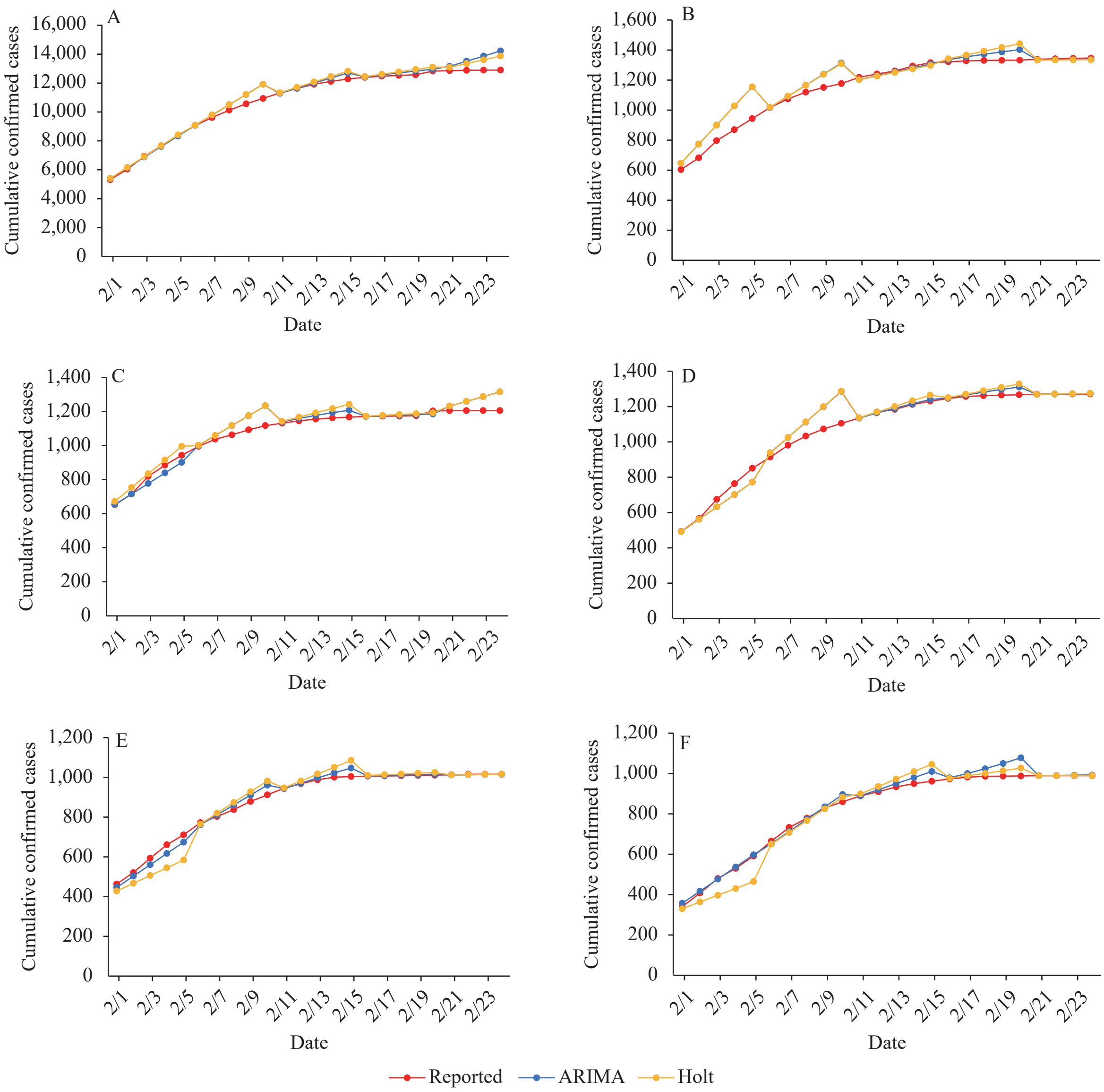

FIGURE 1. Comparison between reported and predicted numbers of COVID-19 in the preceding 5 days using ARIMA model and Holt model in the mainland of China (except Hubei) (A), Guangdong (B), Zhejiang (C), Henan (D), Hunan (E), and Anhui (F).
Abbreviations: COVID-19=Coronavirus disease 2019; ARIMA=autoregressive integrated moving average model; Holt=Holt exponential smoothing model.

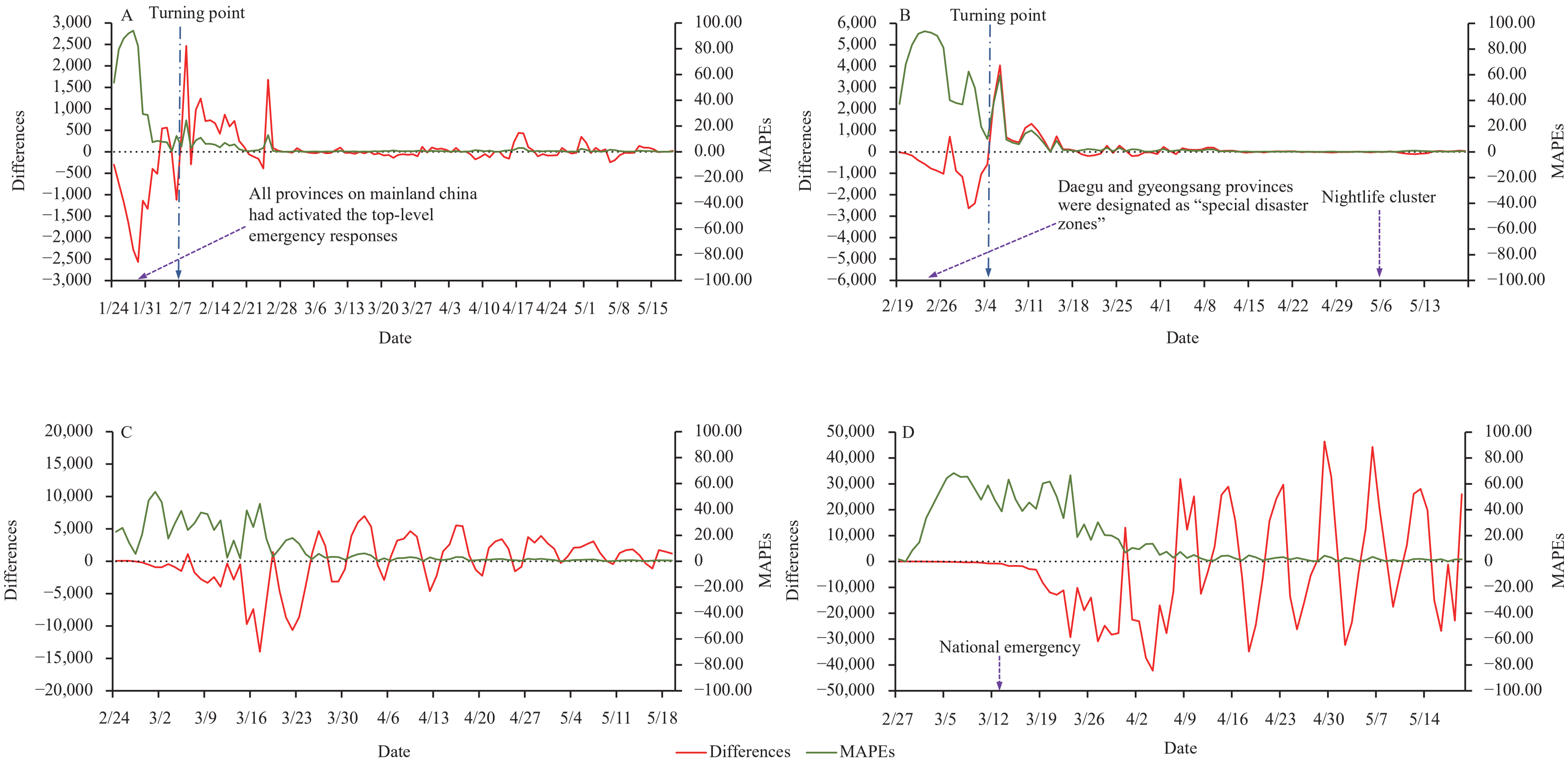

FIGURE 2. Differences and MAPEs (%) between reported and predicted numbers of daily COVID-19 cumulative confirmed cases in the mainland of China (A), Republic of Korea (B), Italy (C), and the United States (D).
Abbreviations: COVID-19=corona virus disease 2019; MAPEs=mean absolute percentage errors; Differences: the predicted number minus the reported number.

China, March 5 in Republic of Korea, and April 27 in Italy. However, the predicted versus observed differences still fluctuated between positive and negative values in the US as of May 19.

DISCUSSION

This study initiated a new framework for epidemic trend analysis by focusing on short-term prediction and real-time recalibrated modeling. Prospectively, the ARIMA model accurately predicted the number of cumulative cases over a 5-day prediction time span. Compared to the Holt model, the ARIMA model has its merits in more accurate predictions, especially during the early epidemic period when the trend was less stable, and the training data was insufficient. Retrospectively, the model can be applied to evaluate whether or not and when the intervention measures had taken effect and to detect the occurrences of abnormal incidents and whether the incidents' effect had lasted by analyzing the pattern of differences between the predicted and observed trends. For China, Republic of Korea, and Italy, the predicted trend was generally lower than the observed trend before a certain date but were higher than or almost in accordance with the observed trend after that date. This alteration potentially reflected the infection control intervention effects. The Chinese government started to enact a series of infection control measures and implemented travel bans and urban transportation suspensions in Wuhan (*7*), and as of January 29, 2020, all provincial-level administrative divisions in the mainland of China had activated the top-level emergency responses to COVID-19 (*8*). Similarly, a series of measures were conducted in Republic of Korea since the first imported case was confirmed. In Italy, intensive and strict measures were implemented in late February and early March. Considering the incubation period and the latent effect, the intervention effect started to be sensible around February 7 in China, March 5 in Republic of Korea, and April 27 in Italy. Considering the time between the intervention starting point and the effect point, China had the shortest interval to reach the point of effect and was followed by the Republic of Korea.

In addition, we noticed several abnormal trend changes. For example, the observed trends slightly exceeded the predicted trends in the last several days after a considerably stable period in the Republic of Korea (Figure 2). Further investigation revealed that this fluctuation might be related to a reported cluster of cases in a popular nightlife district (*9*).

This study was subject to some limitations. Since the ARIMA modeling must be based on sufficient training data, the short-term prediction is not applicable when the epidemic just started, and time series data were lacking. The model performance may vary based on the reliability and diverse epidemic characteristics in different regions; therefore, the generalizability of the model may be limited to some degree. As such, we recommend that real situation should be fully considered before applying.

Above all, the real-time recalibrated modeling method has its merits in capturing the dynamic nature of the epidemic and providing time sensitive information to guide public health responses to COVID-19.

Conflicts of interest: The authors who have taken part in this study declared that they did not have any potential conflicts of interest.

Funding: Zhejiang University special scientific research fund for COVID-19 prevention and control (2020XGZX003), Zhejiang Provincial Innovation Team (2019R01007), Zhejiang Province Key Laboratory (2020E10004), Zhejiang Provincial Natural Science Foundation (LEZ20H260002).

doi: 10.46234/ccdcw2021.112

Corresponding author: Xifeng Wu, xifengw@zju.edu.cn.

[1] Center of Clinical Big Data and Analytics, Second Affiliated Hospital and Department of Big Data Health Science School of Public Health, Zhejiang University School of Medicine, Hangzhou, Zhejiang, China; [2] National Institute for Data Science in Health and Medicine, Hangzhou, Zhejiang University, Zhejiang, China; [3] Department of Surgical Oncology, Affiliated Sir Run Run Shaw Hospital, Zhejiang University School of Medicine, Hangzhou, Zhejiang, China.
[&] Joint first authors.

Submitted: February 22, 2021; Accepted: April 15, 2021

REFERENCES

1. WHO. Listings of WHO's response to COVID-19. 2020. https://www.who.int/news/item/29-06-2020-covidtimeline.[2021-1-14].
2. Wang HW, Wang ZZ, Dong YQ, Chang RJ, Xu C, Zhang SX, et al. Phase-adjusted estimation of the number of coronavirus disease 2019 cases in Wuhan, China. Cell Discov 2020;6(1):10. http://dx.doi.org/10.1038/s41421-020-0148-0.
3. Yang ZF, Zeng ZQ, Wang K, Wong SS, Liang WH, Zanin M, et al. Modified SEIR and AI prediction of the epidemics trend of COVID-19 in China under public health interventions. J Thorac Dis 2020;12(3):165 – 74. http://dx.doi.org/10.21037/jtd.2020.02.64.
4. Health Commission of Hubei Province. The epidemic of novel coronavirus in Hubei province on February 13, 2020. 2020. http://wjw.hubei.gov.cn/bmdt/ztzl/fkxxgzbdgrfyyq/xxfb/202002/t20200214_2027190.shtml. [2021-2-2]. (In Chinese).
5. University JH. COVID-19 dashboard by the center for systems science and engineering (CSSE) at Johns Hopkins University (JHU) 2021.

https://www.arcgis.com/apps/opsdashboard/index.html#/bda7594740fd40299423467b48e9ecf6. [2021-6-1].
6. Hyndman RJ, Khandakar Y. Automatic time series forecasting: the forecast package for R. J Stat Softw 2008;27(3):1 – 23. http://dx.doi.org/10.18637/jss.v027.i03.
7. Health Commission of Hubei Province. Notice of the headquarters for the control and treatment of the epidemic caused by the novel coronavirus in Hubei (No. 1). 2020. http://www.gov.cn/xinwen/2020-01/23/content_5471751.htm. [2021-1-29]. (In Chinese).
8. China Daily. 'Ambitious' response to epidemic receives praise. 2020. http://en.nhc.gov.cn/2020-03/02/c_77181.htm. [2021-1-14].
9. Mitra S. South Korea: 101 coronavirus cases linked to nightclub cluster. 2020. https://www.republicworld.com/world-news/rest-of-the-world-news/south-korea-reports-101-coronavirus-cases-linked-to-nightclub-cluster.html.[2020-5-30].

Methods and Applications

A Longitudinal Cohort Study Using a Modified Child-Pugh Score to Escalate Respiratory Support in COVID-19 Patients — Hubei Province, China, 2020

Yibai Xiong[1]; Yan Ma[1]; Yaxin Tian[1]; Chi Zhang[2]; Wei Yang[1]; Bin Liu[1]; Lianguo Ruan[3]; Cheng Lu[1,#]; Luqi Huang[4,#]

ABSTRACT

Background: We explored a phenotype of liver dysfunction based on modified Child-Pugh (MCP) with coronavirus disease 2019 (COVID-19) and evaluated its relationship with escalation of respiratory support and survival.

Methods: This was a retrospective cohort study involving COVID-19 in-patients at the Wuhan Jinyintan Hospital. This study was performed between January 24, 2020 and March 31, 2020. Escalation of respiratory support and survival were evaluated. Furthermore, the trajectory of liver function was delineated considering the risk of escalation of respiratory support and survival using multilevel logistic regression.

Results: A total of 298 patients were enrolled in this study. A higher proportion of patients with MCP-B on admission exhibited an escalated respiratory support (26 of 55; 47.3%) when compared to patients with MCP-A (9 of 62; 14.5%), indicating that MCP-B was strongly associated with escalation of respiratory support [adjusted hazard ratio (HR): 4.530; 95% confidence interval (CI): 2.060–9.970; P<0.001]. Among the patients on escalated respiratory support, 5 (55.6% of 9) patients with MCP-A died compared to 10 (38.5% of 26) of the patients with MCP-B. Patients with a history of liver disease had a higher mortality risk (adjusted HR: 7.830; 95% CI: 1.260-48.420).

Conclusion: MCP is efficient at stratifying liver dysfunction levels in COVID-19 patients and is strongly associated with escalation of respiratory support.

INTRODUCTION

Liver dysfunction is an independent risk factor for organ dysfunction in coronavirus disease 2019 (COVID-19) patients (*1*). Given the high mortality rate associated with COVID-19, it has not been established which liver dysfunction groups are at higher risk.

The criteria for evaluation of liver dysfunction in COVID-19 patients are incompletely defined. Previous studies have reported independent associations between liver functions and disease progression (*2*). The Child-Pugh score is a classic tool for evaluating liver dysfunction levels (*3*). However, it has some limitations. Evaluation of ascites and hepatic encephalopathy are subjective to some degree. Moreover, there is a causal relationship between ascites and hypoalbuminemia that if determined at the same time, would lead to a bias. Therefore, an objective, recognizable method for evaluating liver dysfunction in COVID-19 patients is crucial. Based on evidence from previous studies (*4–6*), discussion with hepatologists, and our observation that changes in aspartate aminotransferase and gamma glutamyl transpeptidase levels are not clinically significant (*7*), we modified the Child-Pugh score. Furthermore, elevations in lactate dehydrogenase levels are not significant in COVID-19 progression while elevations in aspartate aminotransferase levels are strongly associated with increased neutrophil counts and decreased lymphocyte counts, indicating the severity of viral pneumonia (*4*). Therefore, we replaced ascites with aspartate aminotransferase and defined its cut-off value as 1.5 times the upper limit of normal [<35 IU/L, 1 points; 35–87.5 IU/L, 2 points; >87.5 IU/L, 3 points (35 IU/L is the standard value in Jinyintan Hospital)] in the modified Child-Pugh (MCP) score as a new evaluation of liver dysfunction in COVID-19 patients. This cutoff value was established based on previous studies (*8–9*). In this study, we aimed to assess the impact of liver dysfunction stratification in COVID-19 by evaluating longitudinal associations between MCP and escalated respiratory support.

METHODS

Study Design and Participants

This was a retrospective longitudinal cohort study involving COVID-19 patients that were confirmed by reverse transcriptase polymerase chain reaction (RT-PCR), based on the Chinese diagnosis and treatment protocol for COVID-19 (Trial Version 7) (*10*) admitted at the Jinyintan Hospital. Epidemiological, clinical, and laboratory data for patients were collected between January 24, 2020 and March 31, 2020, at which point patients were admitted and no more patients were admitted. Individuals who were 18 years of age or older, and who tested positive for COVID-19 by real-time RT-PCR were included in this study. No exclusion criteria were applied.

Data Collection

Nose and throat swab specimens or nasopharyngeal aspirates collected from patients were tested for COVID-19 using RT-PCR. Epidemiological information, medical history, and clinical symptoms were recorded upon admission. Imaging and laboratory tests were routinely performed for all patients. Data were extracted from hospital information systems (HISs) using a standardized data collection form. All data were recorded daily. A group of experienced physicians determined the frequency of examinations and then reviewed and cross-checked the data. Implausible values for variables were identified with the data entry department and confirmed by physicians.

Definition

An axillary temperature of at least 37.3 °C was considered as fever. The six-point ordinal scale of clinical status for respiratory support was categorized as follows: 1) 6 points, death; 2) 5 points, need for invasive ventilator; 3) 4 points, high flow humidification oxygen/high frequency oxygen/non-invasive ventilator are needed; 4) 3 points, low flow (1 liters – 5 liters per minute) face mask/nasal cannula for oxygen inhalation; 5) 2 points, oxygen saturation of above 93 without oxygen inhalation; 6) 1 point, discharge (*11*). Mild illness was defined as 2 points, while severe illness was defined as 3 points or above. Escalation of respiratory support was defined as a transition from 2 or 3 points to 4 points or higher.

Chest x-ray and chest computed tomography abnormality (CXR): 0, bilateral pneumonia with no abnormal lesions (unilateral or bilateral pneumonia); 1, unilateral pneumonia with multiple mottling and ground-glass opacity; 2, bilateral pneumonia with multiple mottling and ground-glass opacity.

The practical definition of liver dysfunction was modified from studies on the Child-Pugh score, and other studies that reported that liver dysfunction is highly correlated with COVID-19 progression and associated mortality (*12–14*). The MCP was defined as follows (Table 1): Aspartate aminotransferase (AST) (U/L): <35, 1 point; 35–70, 2 points; >70, 3 points (35 U/L is the normal standard in Jinyintan Hospital). Total bilirubin (TBIL) (μmol/L): <34, 1 point; 34–51, 2 points; >51, 3 points. Albumin (ALB)(g/L): >35, 1 point; 28–35, 2 point; <28, 3 points. Prothrombin time (PT) (s): prolong <4, 1 point; 4–6, 2 points; >6, 3 points. It was graded as 5 points or below for Child-Pugh-A; 6–9 points for Child-Pugh-B; and 10–15 points for Child-Pugh-C. The AST cut-off values were obtained from literature reviews (*8,15–16*) and extensive discussion with hepatology experts and infectious disease specialists.

Statistical Analysis

Categorical and continuous variables were presented as percentages (%) and as means [95% confidence interval (CI)], respectively, while normally distributed data were presented by their medians [interquartile range (IQR)]. For normally distributed data, independent t tests were performed to compare means between two groups for continuous variables; otherwise, the Mann-Whitney test was used. For

TABLE 1. Modified Child-Pugh scoring system.

Item	Score		
	1	2	3
Total bilirubin, mmol/L	<34	34−51	>51
Albumin, g/L	>35	28−35	<28
Aspartate aminotransferase, U/L	<35	35−70	>70
Prothrombin time prolongation, s	<4	4−6	>6

categorical variables, we used Pearson's chi-squared test or Fisher's exact test to determine significant differences.

Probability of escalation was calculated using Kaplan-Meier curves with death or escalation up to 2 points or above as events, and surviving patients recorded in 30 days. Longitudinal analysis was performed using scatterplots of daily results against time, which was visualized by the estimated survival time distribution plot. The Cox regression model was used to simultaneously evaluate the relationship between various risk factors and survival time of patients while the log-rank test was used to determine whether differences in survival rates were statistically significant. Missing data were carried by results from the previous day and only estimated for the repeated measures multivariate model. If more than one result was recorded on a certain day, the most deviated result was chosen to reveal the reality of availability of given information to a clinician at a random time. A locally estimated scatterplot smoothing (LOESS) curve showing 95% CIs for the daily mean was used to present dynamic changes in liver function markers based on the severity of COVID-19 (default settings with a polynomial degree of 2, Gaussian kernel, and interpolation on cell size of 0.2). The mixed-effect Cox proportional hazards regression models were used to establish the factors that were associated with escalation of respiratory support or mortality. A two-sided α of <0.05 was considered statistically significant. All analyses were performed using R statistical software (version 3.6.2; The R Foundation for Statistical Computing, Vienna, Austria)

RESULTS

Patient Population

Out of the 307 patients, 9 patients were excluded because of missing data. Baseline characteristics of this study are summarized in the appendix (Supplementary Table S1 available in http://weekly.chinacdc.cn/). The median age was 60 years (IQR: 49–68), 166 (55.70%) participants were male while 132 (44.30%) participants were female. A total of 112 patients (37.58%) had extra oxygen supply, while 186 (62.42%) only had occasional oxygen inhalation. Among them, 6 (2.0%) patients had fatty liver disease while 10 (3.4%) had viral hepatitis.

Association Between Liver Dysfunction and Escalation of Respiratory Support

After admission, 35 patients were eligible for escalation of respiratory support. Among them, 30 patients were originally included in the severe group while the remaining 5 patients were in the mild group. Since the severe group had higher probability for escalated respiratory support, the study compared liver function among patients who were eligible for escalation of respiratory support and those who were not eligible in the severe group. Because patients in severe group tended to be eligible for escalation, AST levels were highly elevated in the escalation group (Supplementary Table S2 available in http://weekly.chinacdc.cn/).

Then, the trajectory of liver function was assessed in severe patients, which were divided by two groups: the escalated group included escalated patients, while the mend group included patients in stable condition. The LOESS model was used to show the trajectory of ALB, AST, TBIL, and PT in the escalated and mend groups. There were low ALB levels, significant elevated AST levels, higher TBIL levels, and first lower but delayed marked PT (Figure 1). Upon admission, MCP levels were elevated in patients that were eligible for escalation than in those who were not, as determined by the mixed-effects Cox model. Age, gender, comorbidity, and drug were adjusted as confounders [adjusted hazard ratio (HR): 4.530; 95% CI: 2.058–9.970; *P*<0.001] (Figure 2).

A total of 62 (53.0%) patients met the MCP-A level criteria, among whom 9 (14.5%) patients needed escalation; 55 (47.0%) patients met the MCP-B level criteria, among whom 26 (47.3%) patients needed escalation. For the MCP-B patients, after adjusting for age, sex, comorbidity, and drug usage, escalation time was shorter when compared to MCP-A patients (likelihood ratio test *P*<0.001) (Figure 3).

The Association Between Modified Child-Pugh Score Levels and Mortality

Among the 35 patients that were eligible for escalated respiratory support, 20 survived and were discharged. Baseline laboratory results are summarized in the appendix (Supplementary Table S3 available in http://weekly.chinacdc.cn/). Patients that were eligible and survived were younger (61.33 years old), had a shorter PT (11.25 s), and elevated ALB levels

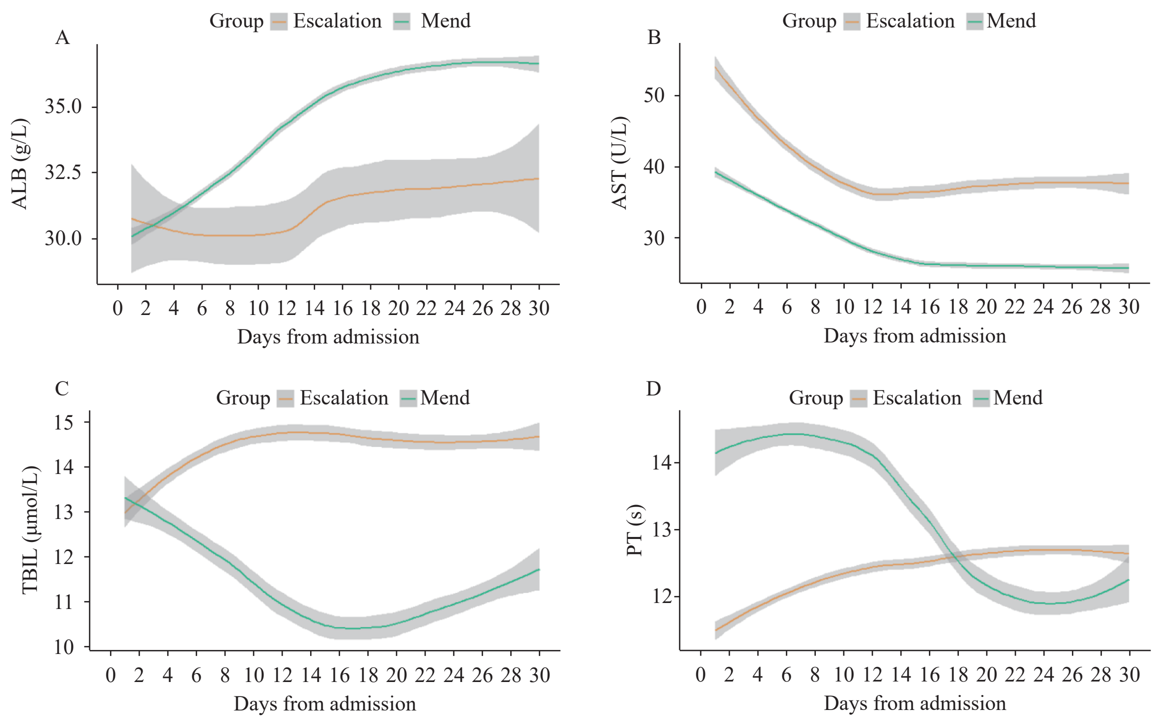

FIGURE 1. Longitudinal laboratory findings of liver function based on a MCP score in escalated respiratory support patients. (A–D) Laboratory results (ALB, AST, TBIL, and PT) based on the MCP score plotted against time with 95% confidence interval, which were fitted by locally estimated scatterplot smoothing curves. Worst daily mean values for all the escalated respiratory support patients were provided, and missing data were imputed from the last day valued. Laboratory results for the escalated respiratory support patients were stratified within 30 days of admission.
Abbreviations: MCP=modified Child-Pugh; ALB=albumin; AST=aspartate aminotransferase; TBIL=total bilirubin; PT=prothrombin time.

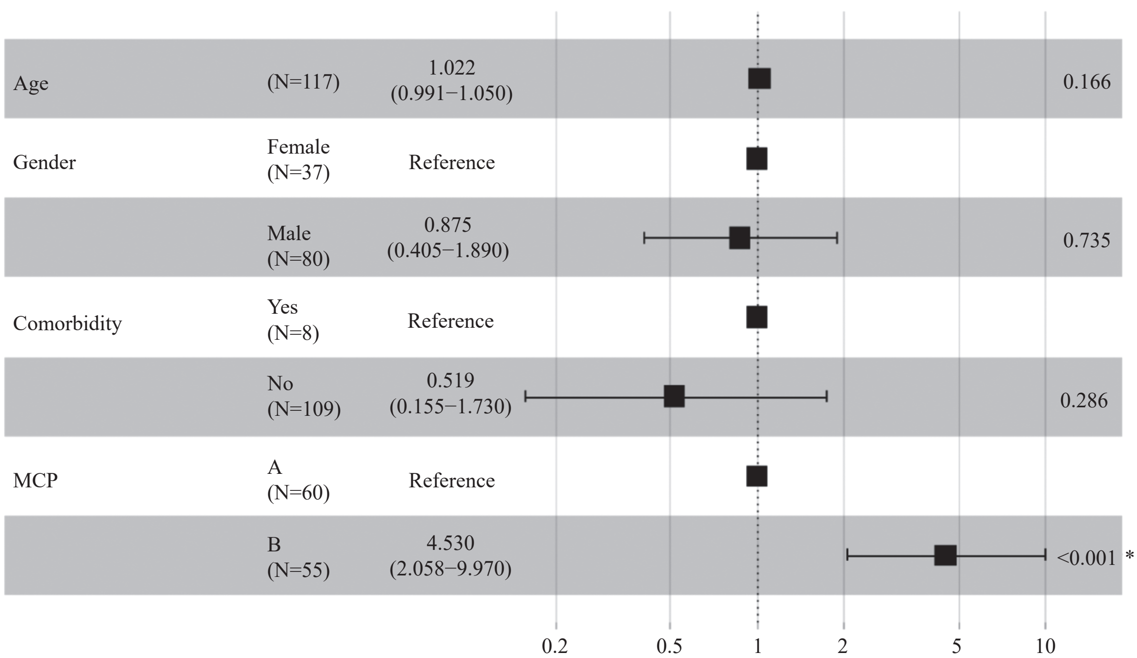

FIGURE 2. Associations between modified Child-Pugh (MCP) score level and escalated respiratory support.
*: The *P* value is statistically significant.

(31.45 g/L).

A total of 9 (25.7%) patients met the MCP-A criteria upon admission while 26 (74.3%) patients met the MCP-B criteria. Overall, 5 (55.6%) patients in the MCP-A group did not survive, which was higher than the 10 (38.5%) in the MCP-B that did not survive. When analyzed using the mixed-effects Cox model, patients without liver disease comorbidities (adjusted HR: 0.128; 95% CI: 0.021–0.791; *P*=0.027) and that were male (adjusted HR: 0.176; 95% CI: 0.052–0.595; *P*=0.005) exhibited better survival probabilities (Figure 4).

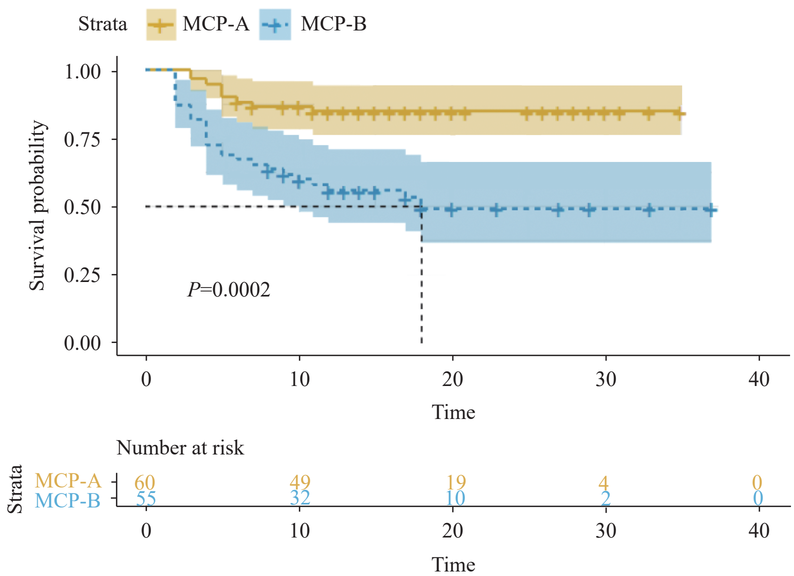

FIGURE 3. Liver dysfunctions based on modified Child-Pugh (MCP) score and escalation-free survival.
Kaplan-Meier analysis of escalation-free survival in severe patients that were in need of extra oxygen support (3 points or above) within 30 days were plotted from the day of admission of every patient. Patients were stratified by which level they met the MCP score criteria. Predicted median survival is shown by the dashed line in the group with MCP-B level.

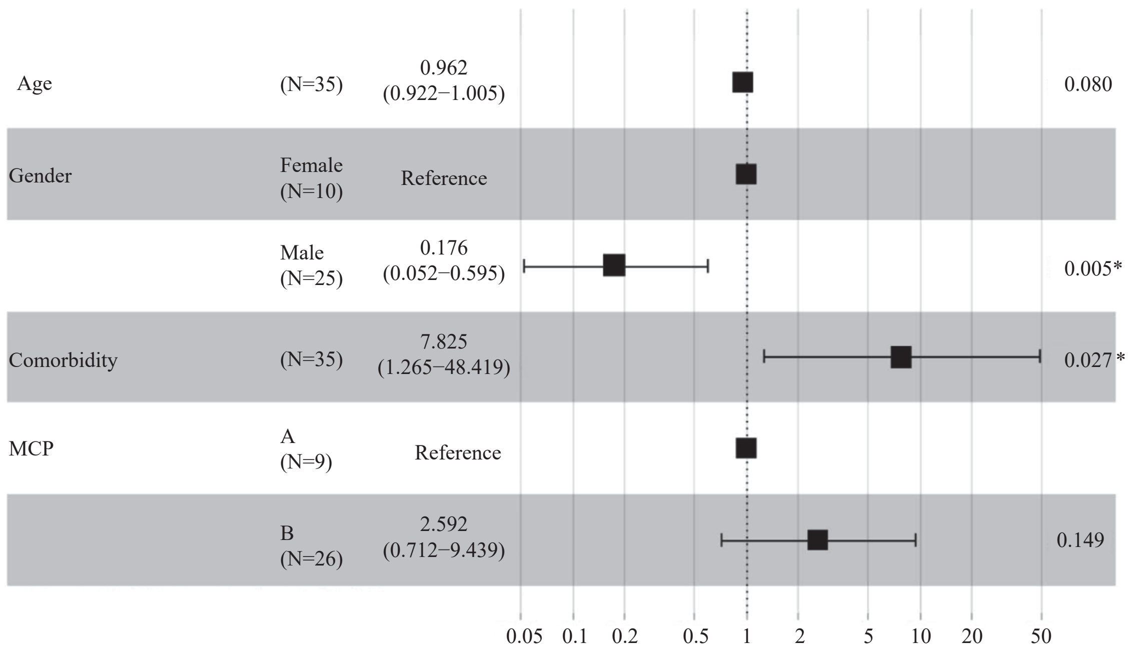

FIGURE 4. Associations between modified Child-Pugh (MCP) score level and mortality
*: The *P* value is statistically significant.

DISCUSSION

In this study, many patients with liver dysfunctions could be stratified based on MCP, which was closely associated with escalation of respiratory support during hospitalization. In the severe group, 47.0% of patients met the MCP-B criteria with 47.3% of them being put on escalated respiratory support.

Among the escalated patients, 74.3% were MCP-B while 25.7% were MCP-A. Eventually, lower proportions (MCP-B: 38.5%; MCP-A: 55.6%) survived. The exact reason could not be established but might be correlated with the standard of care as well as liver and multiorgan dysfunction. Moreover, it could be that more care was emphasized on severe liver dysfunction patients. In addition, liver disease comorbidity is a risk factor for escalated patients.

The association between longitudinal laboratory outcomes and clinical outcomes was also determined. Notably, at admission, elevated AST levels were frequent and more significant than increased PT in escalated patients (*9*). In addition, patients that were eligible for escalation had relatively the same ALB and TBIL levels upon admission, but a contradictory change was found as disease progressed, compared to those who were not eligible for escalation. Eligible patients had low ALB levels and elevated TBIL levels (*7*).

This study was subject to some limitations. The main limitation of this study is that it is single-center study that does not represent diverse group patients. Another limitation was that we used the last values of laboratory results to impute missing data, which could be a potential source of bias. Each patient was prescribed antibiotics, antivirals, and corticosteroids during treatment. Our data could not show the effects of the drugs for liver damage; however, drug-related liver dysfunctions should be evaluated further.

The MCP was associated with escalated respiratory support in COVID-19 patients. Since elevated levels of liver injury indicators were strongly associated with escalation, the MCP criteria should be validated with multicenter, randomized cohorts and monitored during hospitalization.

Acknowledgments: All doctors in Wuhan Jinyintan Hospital.

Conflicts of interest: No conflicts of interest.

Funding: National Science and Technology Major Project (2018ZX10101001-005), China Academy of Chinese Medical Sciences Project (No. 2020YFC0841500).

doi: 10.46234/ccdcw2021.113

[#] Corresponding authors: Cheng Lu, lv_cheng0816@163.com; Luqi Huang, hlq910@126.com.

[1] Institute of Basic Research in Clinical Medicine, China Academy of Chinese Medical Sciences, Beijing, China; [2] Dongzhimen Hospital, Beijing University of Chinese Medicine, Beijing, China; [3] Department of Infectious Diseases, Jinyintan Hospital, Wuhan, Hubei, China; [4] National Resource Center for Chinese Materia Medica, China Academy of Chinese Medical Sciences, Beijing, China.

Submitted: May 03, 2021; Accepted: May 10, 2021

REFERENCES

1. Piano S, Dalbeni A, Vettore E, Benfaremo D, Mattioli M, Gambino CG, et al. Abnormal liver function tests predict transfer to intensive care unit and death in COVID-19. Liver Int 2020;40(10):2394 – 406. http://dx.doi.org/10.1111/liv.14565.
2. Cai QX, Huang DL, Yu H, Zhu ZB, Xia Z, Su YN, et al. COVID-19: abnormal liver function tests. J Hepatol 2020;73(3):566 – 74. http://dx.doi.org/10.1016/j.jhep.2020.04.006.
3. Kambhampati S, Bauer KE, Bracci PM, Keenan BP, Behr SC, Gordan JD, et al. Nivolumab in patients with advanced hepatocellular carcinoma and child-pugh class B cirrhosis: safety and clinical outcomes in a retrospective case series. Cancer 2019;125(18):3234 – 41. http://dx.doi.org/10.1002/cncr.32206.
4. Lei F, Liu YM, Zhou F, Qin JJ, Zhang P, Zhu LH, et al. Longitudinal association between markers of liver injury and mortality in COVID-19 in China. Hepatology 2020;72(2):389 – 98. http://dx.doi.org/10.1002/hep.31301.
5. Mo PZ, Xing YY, Xiao Y, Deng LP, Zhao Q, Wang HL, et al. Clinical characteristics of refractory COVID-19 pneumonia in Wuhan, China. Clin Infect Dis 2020ciaa270. http://dx.doi.org/10.1093/cid/ciaa270.
6. Hundt MA, Deng YH, Ciarleglio MM, Nathanson MH, Lim JK. Abnormal liver tests in COVID-19: a retrospective observational cohort study of 1,827 patients in a major U.S. hospital network. Hepatology 2020;72(4):1169 – 76. http://dx.doi.org/10.1002/hep.31487.
7. de Avelar CR, Pereira EM, de Farias Costa PR, de Jesus RP, de Oliveira LPM. Effect of silymarin on biochemical indicators in patients with liver disease: systematic review with meta-analysis. World J Gastroenterol 2017;23(27):5004 – 17. http://dx.doi.org/10.3748/wjg.v23.i27.5004.
8. Xie KL, Chen CH, Tsai SP, Lu PJ, Wu H, Zeng Y, et al. Loss of life expectancy by 10 years or more from elevated aspartate aminotransferase: finding aspartate aminotransferase a better mortality predictor for all-cause and liver-related than alanine aminotransferase. Am J Gastroenterol 2019;114(9):1478 – 87. http://dx.doi.org/10.14309/ajg.0000000000000332.
9. Chughlay MF, Akakpo S, Odedra A, Csermak-Renner K, Djeriou E, Winnips C, et al. Liver enzyme elevations in *Plasmodium falciparum* volunteer infection studies: findings and recommendations. Am J Trop Med Hyg 2020;103(1):378 – 93. http://dx.doi.org/10.4269/ajtmh.19-0846.
10. National Health Commission of the People's Republic of China. Diagnosis and Treatment Protocol for COVID-19 (Trial Version 7). 2020. http://en.nhc.gov.cn/2020-03/29/c_78469.htm. [2021-3-2]
11. Wang YM, Zhang DY, Du GH, Du RH, Zhao JP, Jin Y, et al. Remdesivir in adults with severe COVID-19: a randomised, double-blind, placebo-controlled, multicentre trial. Lancet 2020;395(10236):1569 – 78. http://dx.doi.org/10.1016/s0140-6736(20)31022-9.
12. Hadid T, Kafri Z, Al-Katib A. Coagulation and anticoagulation in COVID-19. Blood Rev 2020;47:100761. http://dx.doi.org/10.1016/j.blre.2020.100761.

13. Iba T, Levy JH, Connors JM, Warkentin TE, Thachil J, Levi M. The unique characteristics of COVID-19 coagulopathy. Crit Care 2020;24(1):360. http://dx.doi.org/10.1186/s13054-020-03077-0.
14. Wu YY, Li HY, Guo XZ, Yoshida EM, Mendez-Sanchez N, Sandri GBL, et al. Incidence, risk factors, and prognosis of abnormal liver biochemical tests in COVID-19 patients: a systematic review and meta-analysis. Hepatol Int 2020;14(5):621 – 37. http://dx.doi.org/10.1007/s12072-020-10074-6.
15. Medetalibeyoglu A, Catma Y, Senkal N, Ormeci A, Cavus B, Kose M, et al. The effect of liver test abnormalities on the prognosis of COVID-19. Ann Hepatol 2020;19(6):614 – 21. http://dx.doi.org/10.1016/j.aohep.2020.08.068.
16. Zhang GM, Zhang GM, Hu S, Peng YF, Gu B. Is testing of aspartate aminotransferase necessary along with every alanine aminotransferase for health check in elderly individuals? Clin Chim Acta 2020;507:224 – 7. http://dx.doi.org/10.1016/j.cca.2020.05.003.

SUPPLEMENTARY TABLE S1. Clinical characteristics among patients with COVID-19 in the cohort.

Variables	All patients (N=298)	Mild group (N=186)	Severe group (N=112)	*P*
Age, years*	60.00 (49.00, 68.00)	57.00 (46.00, 67.00)	63.00 (56.00, 70.00)	0.001
Gender (Female)†	132 (44.30%)	95 (51.10%)	37 (33.00%)	0.002
Signs and symptoms†				
Fever	92 (31.00%)	61 (33.00%)	31 (27.70%)	0.339
Cough	178 (60.10%)	111 (60.00%)	67 (60.40%)	0.951
Tachypnea	80 (26.90%)	42 (22.70%)	38 (33.90%)	0.035
Muscle soreness	2 (0.70%)	2 (1.10%)	0 (0.00%)	0.530
Headache	3 (1.00%)	3 (1.60%)	0 (0.00%)	0.294
Sore throat	4 (1.40%)	3 (1.60%)	1 (0.90%)	–
Chest pain	1 (0.30%)	1 (0.50%)	0 (0.00%)	–
Diarrhea	5 (1.70%)	3 (1.60%)	2 (1.80%)	>0.999
Nausea and vomiting	3 (1.00%)	2 (1.10%)	1 (0.90%)	>0.999
Comorbidity†				
Cardiovascular diseases	86 (28.90%)	48 (25.80%)	38 (33.90%)	0.134
Digestive system disease	32 (10.70%)	19 (10.20%)	13 (11.60%)	0.707
Endocrine system disease	42 (14.10%)	23 (12.40%)	19 (17.00%)	0.269
Malignant tumor	17 (5.70%)	11 (5.90%)	6 (5.40%)	0.841
Nervous system disease	6 (2.00%)	4 (2.20%)	2 (1.80%)	>0.999
Respiratory system disease	15 (5.00%)	8 (4.30%)	7 (6.20%)	0.456
Vital signs*				
Body temperature, °C	36.70 (36.50, 37.20)	36.70 (36.50, 37.50)	36.60 (36.50, 37.00)	0.635
Heart rate, beats/min	88.00 (80.00, 98.75)	88.00 (80.00, 98.00)	88.00 (84.00, 99.00)	0.231
Respiratory rate, breaths/min	22.00 (20.00, 23.00)	22.00 (20.00, 23.00)	22.00 (20.00, 23.00)	0.088
Systolic blood pressure, mmHg	127.00 (116.00, 138.00)	125.00 (115.00, 136.00)	130.50 (120.00, 138.00)	0.013
Diastolic blood pressure, mmHg	80.00 (74.00, 88.75)	80.00 (73.25, 87.00)	81.50 (74.75, 91.25)	0.437
Laboratory results				
White blood cell count, $\times 10^9$ /L*	5.52 (4.40, 7.50)	5.21 (4.16, 6.65)	6.44 (5.05, 8.99)	<0.001
Neutrophil cell count, $\times 10^9$ /L*	3.77 (2.80, 5.62)	3.34 (2.49, 4.63)	5.10 (3.56, 7.48)	<0.001
Lymphocyte count, $\times 10^9$ /L*	1.08 (0.81, 1.53)	1.24 (0.90, 1.65)	0.90 (0.60, 1.29)	<0.001
Immature granulocyte count*	0.01 (0.01, 0.05)	0.01 (0.00, 0.03)	0.03 (0.01, 0.12)	<0.001
Eosinophils count, $\times 10^9$ /L*	0.03 (0.00, 0.08)	0.03 (0.01, 0.09)	0.02 (0.00, 0.07)	0.167
Hemoglobin, g/L*	126.00 (115.00, 136.00)	123.00 (113.00, 136.00)	128.00 (118.00, 136.00)	0.047
Platelet count, $\times 10^9$ /L*	210.00 (161.00, 272.00)	207.00 (161.00, 271.00)	216.50 (161.75, 279.50)	0.637
IL-6, pg/mL*	8.17 (6.41, 11.83)	7.59 (6.08, 10.95)	9.04 (7.01, 12.84)	0.003
Procalcitonin, pg/mL*	0.04 (0.04, 0.05)	0.04 (0.04, 0.05)	0.04 (0.04, 0.09)	<0.001
Feriritin, ng/mL*	492.02 (252.32, 803.96)	383.04 (194.67, 630.86)	691.96 (450.20, 1,172.65)	<0.001
Erythrocyte sedimentation rate, mm/h*	42.85 (25.00, 61.00)	37.00 (20.00, 54.00)	53.00 (31.00, 66.50)	<0.001
Amyloid A, mg/L*	142.35 (11.00, 235.43)	54.45 (5.65, 219.48)	180.10 (79.60, 246.14)	<0.001
Fibrinogen, g/L*	3.80 (2.80, 5.00)	3.60 (2.62, 4.40)	22.00 (20.00, 26.75)	<0.001
D-dimer level, mg/L*	0.70 (0.39, 1.57)	0.51 (0.31, 1.03)	1.11 (0.57, 3.82)	<0.001
Prothrombin time, s*	11.30 (10.70, 12.00)	11.20 (10.60, 11.75)	11.70 (10.83, 12.60)	<0.001

TABLE S1. (Continued)

Variables	All patients (N=298)	Mild group (N=186)	Severe group (N=112)	*P*
Prothrombin activity, %*	102.70 (89.00, 121.90)	108.10 (93.30, 124.30)	96.20 (77.95, 118.30)	<0.001
International normalized ratio*	0.97 (0.91, 1.02)	0.96 (0.90, 1.01)	0.99 (0.92, 1.06)	0.004
Activated partialthromboplastin time, s*	26.50 (23.30, 30.50)	25.95 (23.40, 29.70)	27.10 (23.20, 31.10)	0.508
Albumin, g/L§	33.14 (4.64)	34.76 (4.37)	30.45 (3.77)	<0.001
Aminotransferase alanine, U/L*	32.00 (20.00, 50.00)	28.50 (18.75, 45.00)	38.00 (23.00, 54.00)	0.005
Aminotransferase aspartate, U/L*	32.00 (24.00, 45.00)	29.00 (23.00, 41.00)	37.00 (29.00, 56.00)	<0.001
Total bilirubin, mmol/L*	12.85 (9.67, 16.50)	13.10 (9.70, 16.70)	12.00 (9.20, 16.15)	0.186
Indirect bilirubin, mmol/L*	8.35 (6.20, 11.43)	8.80 (6.80, 11.70)	7.80 (5.65, 10.70)	0.035
Direct bilirubin, mmol/L*	4.10 (3.00, 5.20)	4.00 (2.90, 5.12)	4.10 (3.20, 5.38)	0.440
Lactate dehydrogenase, U/L*	257.00 (197.50, 350.50)	225.00 (180.00, 277.00)	339.50 (261.00, 451.75)	<0.001
Alkaline phosphatase*	76.00 (60.00, 93.25)	76.00 (60.00, 94.00)	75.00 (60.00, 93.00)	0.984
Creatinine, μmol/L*	67.40 (57.00, 80.25)	66.50 (56.00, 78.00)	70.10 (59.00, 83.55)	0.039
Blood urea nitrogen, mmol/L*	4.40 (3.46, 5.43)	4.00 (3.30, 5.00)	4.90 (3.95, 6.55)	<0.001
Neutrophil to lymphocyte ratio*	5.5 (4.8, 6.3)	8.0 (6.6, 9.3)	3.7 (3.1, 4.3)	<0.001
CXR†,¶	297	186	111	
0	91 (30.63%)	74 (39.78%)	17 (15.32%)	<0.001
1	21 (7.11%)	19 (10.22%)	2 (1.80%)	0.227
2	185 (62.29%)	93 (50.00%)	92 (82.89%)	<0.001
Blood oxygen saturation†,¶	276	186	90	<0.001
2	186 (67.39%)	186 (100%)	0 (0%)	
3	4 (1.45%)	0 (0%)	4 (4.44%)	
4	78 (28.26%)	0 (0%)	78 (86.67%)	
5	8 (2.90%)	0 (0%)	8 (8.89%)	

Notes: *P* values were calculated by Pearson's chi-squared test or fisher's exact test for Count Data, and t test or Mann-Whitney test, as appropriate. *P* values denoted the comparison among mild group and severe group. Some *P* values were not given (denoted "−") due to insufficient number of cases.

Abbreviations: CXR=Chest x-ray and chest computed tomography abnormality.

*: median (interquartile range, IQR);

†: n/N (proportion, %);

§: mean (standard deviation, SD);

¶: due to missing values, number of patients are different from the overall number.

SUPPLEMENTARY TABLE S2. Baseline of liver function in patients who were eligible for escalation.

Variables	Total (N=117)	Escalation (N=35)	Mend (N=82)	*P*
Gender (female)†	37 (31.60%)	10 (28.60%)	27 (32.90%)	0.643
Age, years§	61.74 (12.48)	62.71 (12.58)	61.33 (12.49)	0.587
Comorbidity†	8 (6.80%)	3 (8.60%)	5 (6.10%)	0.694
Prothrombin time, s*	11.70 (10.80, 12.60)	11.70 (10.85, 12.75)	11.70 (10.80, 12.60)	0.711
Albumin, g/L*	30.30 (28.05, 32.92)	29.60 (28.20, 32.45)	30.30 (27.90, 33.20)	0.701
Aminotransferase aspartate, U/L*	37.50 (29.00, 56.00)	53.00 (38.00, 62.00)	33.00 (26.00, 49.00)	<0.001
Aminotransferase alanine, U/L*	38.50 (24.00, 55.00)	39.00 (25.50, 56.00)	38.00 (22.00, 53.00)	0.729
Total bilirubin, mmol/L*	12.05 (9.25, 16.07)	11.90 (9.85, 16.40)	12.10 (9.10, 15.60)	0.714
Modified Child-Pugh†,¶	115	35	80	<0.001
A	60 (52.17%)	9 (25.71%)	51 (63.75%)	
B	55 (47.83%)	26 (74.29%)	29 (36.25%)	
C	0 (0)	0 (0)	0 (0)	

Notes: *P* values were calculated by Pearson’s chi-squared test or fisher’s exact test for Count Data, and t test or Mann-Whitney test, as appropriate. *P* values denoted the comparison among escalation group and mend group.

*: median (interquartile range, IQR);

†: n/N (proportion, %);

§: mean (standard deviation, SD);

¶: due to missing values, number of patients are different from the overall number.

SUPPLEMENTARY TABLE S3. Baseline of liver function in patients who survived or not from the escalation.

Variables	Total (N=35)	Death (N=15)	Survived (N=20)	*P*
Gender (female)†	10 (28.60%)	3 (20.00%)	7 (35.00%)	0.643
Age, years§	61.74 (12.48)	62.71 (12.58)	61.33 (12.49)	0.587
Comorbidity†	3 (8.60%)	1 (6.70%)	2 (10.00%)	0.694
Prothrombin time, s*	11.70 (10.85, 12.75)	12.90 (11.70,13.70)	11.25 (10.40, 12.05)	0.004
Albumin, g/L*	29.60 (28.20, 32.45)	28.60 (27.10, 29.95)	31.45 (29.10, 34.25)	0.002
Aminotransferase aspartate, U/L*	53.00 (38.00, 62.00)	54.00 (38.50, 57.00)	51.00 (38.00, 64.25)	0.894
Aminotransferase alanine, U/L*	39.00 (25.50, 56.00)	30.00 (22.50, 44.00)	47.00 (32.00, 58.75)	0.147
Total bilirubin, mmol/L§	13.59 (5.81)	15.69 (7.16)	12.02 (4.07)	0.089

Notes: *P* values were calculated by Pearson’s Chi-squared test or Fisher’s Exact test for Count Data, and t test or Mann-Whitney test, as appropriate. *P* values denoted the comparison among death group and survived group.

*: median (interquartile range, IQR);

†: n/N (proportion, %);

§: mean (standard deviation, SD).

Outbreak Reports

Investigation of Brucellosis Caused by Raw Goat Milk — Fujian Province, China, April–June, 2019

Mu Di[1,2,&]; Zhongfa Tao[1,2,3,&]; Weiping Hua[4]; Jiandong Chen[4]; Jingming Cao[4]; Yanqin Deng[5]; Huihui Liu[2]; Lijie Zhang[2]; Yishan Chen[6]; Qiulan Chen[1]; Wenwu Yin[1,#]

Summary

What is already known about this topic?

Brucellosis is one of the most important zoonotic diseases in China. Goat milk and dairy products are essential pathways for foodborne transmission of brucellosis. Pasteurization can completely kill *Brucella* spp. in milk, and milk-borne transmission is mainly related to unhealthy dietary hygiene habits and insufficient epidemic control among animals.

What is added by this report?

This epidemic is the first outbreak of brucellosis in Zhangping City, Fujian Province. A total of 6 confirmed cases were found, and the onset time was from April to June 2019. The investigation suggested that the transmission chain of the epidemic included a private butcher, an infected goat from the north, a dairy farmer, close contact spread, unsterilized goat milk, and consumers drinking raw goat milk.

What are the implications for public health practices?

For the non-endemic area of brucellosis, preventing the import of infected animals and enhancing the practitioner's and the public's awareness of disease prevention has important public health significance. It is necessary to strengthen the transregional quarantine of livestock, the food safety inspection and management, and the practitioners' and public's awareness of food safety.

On July 3, 2019, Zhangping City reported an outbreak of brucellosis in a family cluster. The patients were a mother and a daughter (Patients I and II). Except for drinking goat milk produced and bottled from a local farmer, there was no other suspected exposure, so foodborne infection was highly likely. The city only reported 1 case of human brucellosis in 2011 (Yongfu County) and 1 case in 2017 (Heping County). Livestock were not routinely vaccinated against brucellosis. After the second reported case in 2017, the municipal-level agricultural department carried out a general investigation of brucellosis among livestock. The targeted prevention and control recommendations were put forward to determine the source of the epidemic and risk factors, and onsite investigations were carried out.

INVESTIGATION AND RESULTS

The suspected case definition was as follows: onset of patient illness occurred during the period from January 1 to July 3, 2019; residents of Zhangping City with fever, hyperhidrosis, muscle or joint pain, or fatigue; patient symptoms might be accompanied by liver, spleen, lymph nodes, testicular swelling, and other manifestations; and the rose Bengal test (RBT) result was positive. The confirmed case definition was as follows: a serum (tube) agglutination test (SAT) of titer ≥1∶100; or a suspected case with isolated *Brucella* from the patient's blood, bone marrow, other body fluids, and excrement by bacterial isolation and culture. The recessive infection definition: RBT was positive but no clinical manifestations were detected.

Case searching was performed by acquiring case records, laboratory test reports, and interviews in local hospitals. Blood samples were taken from the dairy farmer (Mr. C) suspected of producing the goat milk that led to this outbreak, Mr. C's family members, and those who had drunk goat milk from Mr. C's farm between January 1 and July 3, 2019. In addition, further investigations were conducted into the hygiene habits of goat milk consumers; the breeding and quarantine of pigs, cattle, and goats in Zhangping City; the processing and supply of dairy products in Heping County; and sampling and quarantining the milk goats in Heping County.

If a RBT-positive person was found during the case search, the detailed demographic data, clinical data, eating habits, occupational history, preventive measures, and exposure history would be collected. If a patient had other suspected exposures, blood samples were tested to identify the source of infection.

A total of 146 persons were sampled during the case search, and 6 confirmed cases were found. One of the blood specimens was cultured as *Brucella ovis*. All patients had symptoms of fatigue, 5 cases (83%) were accompanied by fever, 2 cases (33%) had hyperhidrosis and muscle aches, and 1 case (17%) had vomiting, chills, and headache. There were no severe deaths or recessive infections. The male-to-female ratio was 1∶5, including 3 workers, 2 unemployed houseworkers, and 1 student. The cases were from 4 households, all within the delivery scope of goat milk of Mr. C, and no other epidemiological association was found. Only one patient experienced onset of symptoms in April, and the remaining patients experienced onset from May 27 to June 12.

Except for Patient V who was engaged in pig offal processing, the other patients' only suspected exposure was the raw goat milk (Table 1). The RBT test was negative for Patient V's coworkers and blood samples from the pig offal, which reduced the likelihood of transmission through pig offal processing. A total of 2 private farms in Zhangping City supplied fresh goat milk. Mr. C's dairy farm was a family workshop that did not abide by adequate sanitation measures, and 3 sampling specimens of Mr. C's dairy goats were positive for RBT (++++) while samples from the other dairy farm tested negative, confirming that the source of the infection was the dairy goats from Mr. C's dairy farm.

This epidemic was the first outbreak of brucellosis among livestock in Zhangping City, and further investigations were needed to find the source of the infected dairy goat. The environmental investigation found that Mr. C's dairy farm was a closed iron goat pen so that the goat could not contact other animals. Because Mr. C's goats did not have a quarantine certificate, the infected dairy goat was likely purchased by Mr. C as the last quarantine record of a dairy goat he possessed was in 2014. Mr. C brought dairy goats twice: in 2016, 60 goats were purchased from a neighboring village in Zhangping City; and in 2017, an additional 2 dairy goats were purchased in Zhangping City from Mr. Y, one of which was likely the infected goat. The goats had been slaughtered and sold, and the relevant personnel's serum RBTs were all negative. The dairy goats were still maintained when the outbreak occurred. Mr. C stated that the goats had "slow growth and low milk production." One of the goats gave birth to lambs in early March 2019. The peak of infected milk lamb chops was after lambing (*1*) and combined with the case's onset date and the incubation period of brucellosis. It was speculated that Y's milk goat was the source of infection for this outbreak (Figure 1).

A retrospective epidemiological investigation into the goat producer Mr. Y showed that Mr. Y's goats had their first brucellosis case in Heping City on August 29, 2017. On August 1, 2017, Mr. Y bought 15 goats from a northern region (the specific source is unclear) and contracted brucellosis after slaughtering the goat with his bare hands with palms that had ruptured skin. During the local animal epidemic control department's investigation, Mr. Y had killed or sold most of the goats, and no brucellosis was detected in the remaining 3 dairy goats. During this investigation, Mr. Y admitted that he sold 2 goats to Mr. C before culling by the animal husbandry department to reduce losses. Although the agricultural department carried out a general survey of brucellosis among livestock, his goat farm was not quarantined because Mr. C left the same day. The infected dairy goats were not found.

TABLE 1. Summary of cases in a brucellosis outbreak in Zhangping City, Fujian Province in 2019.

Case number	Suspected exposure	Drinking method	Onset date	Main symptoms	Lab results	
					RBT	SAT*
I (index case)	Goat milk	Warm bath* or direct consumption	June 1	Fever, sweating, fatigue	Positive	1:400
II	Goat milk	Warm bath or direct consumption	June 3	Fever, fatigue	Positive	1:400
III	Goat milk	Warm bath or direct consumption	June 12	Fever, vomiting, fatigue	Positive	1:400
IV	Goat milk	Direct consumption	April 3	Muscle aches, fatigue	Positive	1:100
V	Goat milk and processing pork	Direct consumption	May 27	Fever, muscle aches, sweating, fatigue	Positive	1:200
VI	Goat milk	Warm bath or Direct consumption	June 10	Headache, fever, chills, fatigue	Positive	1:800

Abbreviations: RBT=rose Bengal test; SAT=Serum agglutination test.
* Warm bath: warming up the milk to a suitable temperature by bathing it into warm water.

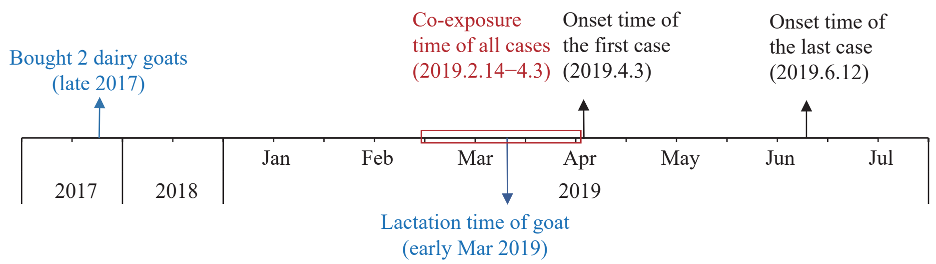

FIGURE 1. Timeline of the dairy farmer, Mr. C, purchasing the brucellosis-infected goats and the incidence of cases in the outbreak in Fujian Province, April–June, 2019.

PUBLIC HEALTH RESPONSE

All dairy goats in Mr. C's farm were culled and buried, and disinfection was conducted for the buildings. Medical institutions at all levels in Zhangping City were trained to strengthen diagnostic capabilities and brucellosis treatment. All goat breeders received health and hygiene education, and local farmers were trained on use of personal protection and the need for goat quarantine, especially to reduce incidence of brucellosis. Residents who consumed goat milk were recommended to monitor symptoms closely for an extended period after the outbreak.

DISCUSSION

In this outbreak investigation, importing an infected goat was the core link that likely caused the local brucellosis outbreak. In recent years, China's brucellosis disease burden had gradually spread from northern pastoral and semi-pastoral areas to southern non-pastoral regions (*2–4*). The main reason could be the increase in livestock trading between the north and south and increased private free-range livestock in the south. But the involved stakeholders' awareness and use of quarantine measures were relatively weak, causing an influx of infected animals and products from north to south (*4*). The investigation found that individual traders did not have compulsory quarantine measures in all aspects of purchasing, breeding, selling, and slaughtering livestock and their biological products. Practitioners had no incentive to submit them for inspection. Therefore, for non-endemic areas, preventing the import of infected animals and strengthening practitioners' and the general public's awareness for disease prevention has significant public health significance. The government should enhance the quarantine of transregional livestock transportation and local disease screening.

Because brucellosis symptoms in livestock are relatively hidden, outbreak control depends more on practitioners' active cooperation. The survey showed that the basic-level goat breeders' main paths for brucellosis prevention were veterinarians, traditional health education materials, and relatives and friends (*5*). Therefore, veterinary departments are encouraged to use their contact with goat breeders to strengthen practitioners' awareness of the effectiveness of quarantine measures for their livestock.

In recent years, food-borne brucellosis had repeatedly occurred in southern China (*6–9*). Contaminated dairy products were an important route of transmission of brucellosis (*9–10*). The interview found that residents in Zhangping City generally believed that raw milk products were more nutritious and were not aware of the possible health risks of raw milk products. As people's awareness of brucellosis was low, governments in low-risk areas should strengthen food safety inspections and management and raise the people's awareness of food safety.

This investigation was subject to some limitations. The local animal epidemic control department did not number when sampling and culling the dairy goat. During this investigation, the disease control agency could not obtain a quality sample from Mr. C's dairy goat. The quality of the blood sample available was poor, and the blood culture did not grow, so the animal disease control department could not obtain etiological evidence of infected dairy goat.

doi: 10.46234/ccdcw2021.111

Corresponding author: Wenwu Yin, yinww@chinacdc.cn.

[1] Chinese Center for Disease Control and Prevention, Infectious Diseases Management Office, Beijing, China; [2] China Chinese Field Epidemiology Training Project, Beijing, China; [3] Guizhou Provincial Center for Disease Control and Prevention, Guiyang, Guizhou, China; [4] Zhangping County Center for Disease Control, Zhangping, Fujian, China; [5] Fujian Provincial Center for Disease Control and Prevention, Fuzhou, Fujian, China; [6] Emory University, Atlanta, USA.
[&] Joint first authors.

Submitted: November 04, 2020; Accepted: April 14, 2021

REFERENCES

1. Li RN, Shu C, Lei LX, Lei LX. Epidemiologic analysis and clinical manifestations of 38 children with brucellosis. Chin J Woman Child Health Res 2019;30(7):892 – 5. http://dx.doi.org/10.3969/j.issn.1673-5293.2019.07.028. (In Chinese).
2. Chen QL. Spatio-temporal analysis of brucellosis in my country and research on the quality of life related to patients' health [dissertation]. Beijing: Chinese Center for Disease Control and Prevention; 2017. http://cdmd.cnki.com.cn/article/cdmd-84501-1017118494.htm. (In Chinese).
3. Shi YJ, Lai SJ, Chen QL, Mu D, Li Y, Li XX, et al. Analysis on the epidemiological features of human brucellosis in northern and southern areas of China, 2015-2016. Chin J Epidemiol 2017;38(4):435 – 40. http://dx.doi.org/10.3760/cma.j.issn.0254-6450.2017.04.005. (In Chinese).
4. Lai SJ, Zhou H, Xiong WY, Yu HJ, Huang ZJ, Yu JX, et al. Changing epidemiology of human brucellosis, China, 1955-2014. Emerg Infect Dis 2017;23(2):184 – 94. http://dx.doi.org/10.3201/eid2302.151710.
5. Liu P, Zeng H, Liu CG, Wang JF, Gao L, Xu QG, et al. The situation and potentially influential factors of brucellosis awareness in occupational groups. Chin J Endemiol 2018;37(9):716 – 20. http://dx.doi.org/10.3760/cma.j.issn.2095-4255.2018.09.007. (In Chinese).
6. Xiang LH, Zhou WZ, Tang FY, Zhu YF, Tan ZM, Liu XY, et al. An outbreak of brucellosis in a village in Jiangsu province. Chin J Epidemiol 2014;35(10):1135 – 7. http://dx.doi.org/10.3760/cma.j.issn.0254-6450.2014.10.013. (In Chinese).
7. Tian GZ, Cui BY, Zhao HY, Jiang H, Piao DR. Studies on epidemiology and molecular characteristics of *Brucella melitensis* during an outbreak of brucellosis. Dis Surveill 2017;32(3):211 – 5. http://dx.doi.org/10.3784/j.issn.1003-9961.2017.03.011. (In Chinese).
8. Qin QC, Li ZJ, Chen XQ, Zhao SY, Cheng GH, Cui BY. Epidemiological investigation of an outbreak of brucellosis caused by drinking of unpasteurized ewe's milk in Hezhou of Guangxi. Dis Surveill 2018;32(8):634 – 7. http://dx.doi.org/10.3784/j.issn.1003-9961.2017.08.006. (In Chinese).
9. Pappas G, Papadimitriou P, Akritidis N, Christou L, Tsianos EV. The new global map of human brucellosis. Lancet Infect Dis 2006;6(2):91 – 9. http://dx.doi.org/10.1016/S1473-3099(06)70382-6.
10. Franco MP, Mulder M, Gilman RH, Smits HL. Human brucellosis. Lancet Infect Dis 2007;7(12):775 – 86. http://dx.doi.org/10.1016/S1473-3099(07)70286-4.

Healthy China

Creating Healthy Enterprises: the Workplace Health Action Plan in China

Yanyan Sun[1]; Xin Sun[1]; Jun Ren[1,#]; Boya Li[1]

Summary

On October 21, 2019, the "*Notice on promoting the healthy enterprises*" and "*Specification of Healthy Enterprise Construction (trial)*" were issued jointly by the National Patriotic Health Campaign Committee Office and six other government partners. As one of the objectives and tasks of the occupational health protection action (2019–2030), this multisectoral "Healthy Enterprise" Action Plan (HEAP) serves as the first "healthy cell" project carried out at the national level as an indispensable part of the Healthy China Initiative and the Healthy City Movement.

It is of great significance to recognize the importance of the burden of disease linked to the exposure of occupational risks and the ability to identify the main areas of concern.

This article interprets the process of how the healthy workplace or healthy enterprise was originated and evolved; how the theory was introduced and developed in China; and how the 4 main action indicators toward healthier and safer workplaces were formulated including the following: 1) developing the health policy system; 2) building healthy working environments; 3) providing health services; and 4) creating healthy culture. It concludes that the national "healthy enterprise" policy is a specific workplace-based public health practice in the field of occupational health and contributes to build a preventive culture in the context of the Healthy China Initiative. It aims to explore and summarize workplace health promotion models, methods, and experience suitable for China and to disseminate them across China.

BACKGROUND OF THE HEALTHY ENTERPRISE ACTION PLAN

In 1995, the World Health Assembly of the World Health Organization (WHO) endorsed the *Global Strategy on Occupational Health for All*, which emphasized the importance of primary prevention of occupational diseases and encouraged countries to establish national policies and programs for occupational health (*1*). However, 10 years later, a national survey revealed that improvements in healthy workplace approaches were minimal and that further improvement was required (*2*). In 2007, the 60th World Health Assembly endorsed the *Global Plan of Action on Workers' Health (GPA), 2008–2017* and set clear objectives and priority areas for action, one of which was to protect and promote health at the workplace (*3*). The *Stresa Declaration on Workers' Health (2006)*, the *ILO Promotional Framework for Occupational Health and Safety Convention (ILO Convention 187) (2006)*, and the *Bangkok Charter for Health Promotion in a Globalized World (2005)* also provided important points of orientation for linking occupational health with public health to achieve a basic level of health for all workers (*2*).

In this context, the WHO provided a flexible framework *Healthy Workplaces: A Model for Action (2010)*, which was adaptable to diverse countries, workplaces, and culture (*4*). At the core of the model is the need to secure the engagement of the workforce via effective leadership and the promotion of workplace culture values that underpin health and wellbeing by considering 4 action areas including the following: 1) the physical work environment; 2) the psychosocial work environment; 3) personal health resources; and 4) enterprise involvement in the community. Since then, numerous groups and networks addressing workplace health have been developed in different regions and countries. The European Network for Workplace Health Promotion provided the definition of "Workplace Health Promotion (WHP)" as "the combined efforts of employees, employers, and society to improve the health and wellbeing of people at work" (*5*). The "Healthy Enterprise" Standard (BNQ9700-800) in Canada specified a series of WHP action plans and recognized the efforts of companies by certifying them to maintain and sustainably improve the health of people in the workplace (*6*). The Total Worker Health approach in the United States was defined as policies, programs, and practices that integrated protection from work-related safety and health hazards with promotion of injury and illness-prevention efforts to advance the wellbeing of the United States workforce (*7*). The Total Health Promotion in Japan was a groundbreaking approach to health promotion theory and practice and aimed to enhance the human experience free from restrictive classifications and false images (*8*).

Since 1993, pilot projects for workplace health practice in different industries and companies have been developed with the support of the WHO. The project has explored and summarized overall intervention strategies of WHP that were verified effectively and suitable in China (*9*). A series of WHP practical tools, including the compilation of regulations, archives, evaluation tools, typical cases, analyses, and health education resources, etc., have been developed for the implementation, assessment, and evaluation of healthy enterprises. Although enormous practices and achievements have been made, numerous problems, including lack of recognition of the importance of occupational disease prevention, inadequate capacity of occupational health services and little funding, have constrained further development of WHP in China. In October 2019, "Healthy Enterprise" Action Plan (HEAP) was issued nationwide with the aim of providing new impetus to move from strategy to action and to shift the pilot exploration to a practical and indispensable part of "Healthy China" and "Healthy City". Recently, experts of China CDC, together with experts of government agencies and other stakeholders, have jointly developed a practical guideline specific for various enterprises, standardizing the following 4 major advocacy action indicators, as listed in Table 1.

MAJOR ACTION INDICATORS AND STRATEGIES OF HEAP

1) Establishing and Improving Health Policy Systems

The HEAP was jointly formulated and published by 7 ministries and commissions of the central government, and a multi-sectoral cooperation mechanism in which each department promotes workers' health collaboratively, and a leading group of national health enterprise construction were established. In line with the administrative impetus provided by the Chinese government to put health in top priority for all policies, policy instruments and mechanisms on workers' health based on the needs identified at the enterprise level must be developed and implemented.

The strategy of HEAP advocates that all components of health systems should be involved in an integrated response to the specific health needs of working populations, particularly the most vulnerable populations, including complying with all legal rules and regulations regarding workplace conditions; raising awareness and introducing more strict regulations, policies, work plans, and systems for controlling and preventing occupational risks in the workplace; and improving abilities of early examination, diagnosis, and treatment of occupational diseases. Furthermore, activities related to workers' health should be planned, implemented, and evaluated. Workers must be responsible for their own health and have a right to be involved at all levels in formulating, supervising, and implementing policies and programs for the establishment and development of healthy enterprises.

2) Building Healthy Working Environments

Recent data from the ILO indicated that the number of work-related deaths increased from 2.33 million in 2014 to 2.78 million in 2017 (*10*). A total of 18 occupational risk factors were measured in the Global Burden of Disease Survey 2016. Only occupational exposure to asbestos decreased, whereas all other exposures increased almost 7% between 1990 and 2016 (*11*). The National Occupational Disease Reporting System noted a total of 23,476 new cases of occupational disease in 2018 (*12*). One occupational disease, pneumoconiosis, is caused by exposure to dust in the workplace and accounted for more than 83% of all the occupational diseases. The report noted

TABLE 1. Major advocacy indicators proposed by the Healthy Enterprise Action Plan.

Action indicators	Major contents
1. Developing health policy systems	Refers to relevant organizations, staffing, funding, and policies; contracts; work injury insurances; and ensuring all staff participation.
2. Building healthy working environments	Including general public area environments; office environments; and the production environments.
3. Providing health services	Refers to general health services (e.g., infectious control, major foodborne diseases control, and regular health check-up especially for female workers); mental health services; and occupational health services.
4. Creating healthy culture	Refers to workplace health promotion; the psychosocial work environment; and social responsibility of enterprises.

relatively new occupational diseases, such as mental and musculoskeletal disorders, to be on the rise. These findings suggested that technological and social changes, along with global economic conditions, were aggravating existing health hazards and creating new issues. In addition, occupational exposure to traditional and well-known risk factors are continuing to increase to a significant degree, and there is still a long way to go before the exposure to occupational risk factors reverses on a global level.

As awareness increases, more urgent and vigorous action is needed to identify the extent of the challenge of occupational diseases and prevent them from taking their toll. HEAP advocates that employers have the primary responsibility to prevent occupational diseases by taking preventive and protective measures through anticipation, recognition, evaluation, and control of risks at work. They need to combine these actions with health surveillance to detect health impacts as early as possible and identify occupational diseases with long incubation periods. In addition, they need to make sure that workplaces are as clean, hygienic, environmentally sound, comfortable, beautiful, and humane as possible.

3) Improving the Performance of and Access to Health Services

Scientific evidence has shown that, in the long term, work-related stress can lead to musculoskeletal disorders, hypertension, and cardiovascular disease. It may also alter immune function, which in turn may facilitate the development of cancer. Work-related stress can lead indirectly to problems inside and outside the workplace. Many harmful effects of lifestyle behaviors, such as smoking, alcohol and drug abuse, malnutrition, and lack of exercise, may interact with workplace hazards (*13*). However, adjusting the content of occupational health services may contribute to the early detection of occupational and noncommunicable diseases, and with appropriate early treatment can decrease mortality and the frequency and extent of disability.

As the role of health services in the Healthy China 2030 (*14*) blueprint is in the transition from basic disease treatment to prevention and health promotion, the strategies of HEAP focus on a new occupational health service paradigm that extends the classical focus on "health risk management," which is workplace hazards and risk to health, including the medical aspects of sickness, absence, and rehabilitation; the support and management of chronic noncommunicable diseases; and the WHP. Employee health programs are encouraged to assist workers to manage their occupational health, prevent chronic diseases, establish healthy behaviors, and become proactive with their healthcare, especially in relation to stress, alcohol and drugs, tobacco, nutrition, and physical activities. Companies dominated by young and middle-aged workers should pay special attention to their workers' mental health and provide psychological health services, such as employee assistance programs.

4) Creating Healthy Culture

The organizational culture refers to the attitudes, values, beliefs, and practices that are demonstrated daily in the enterprise, which affects the mental and physical wellbeing of employees. A successful enterprise is based on people working in it and on its organizational culture. A supportive workplace culture is the foundation of a healthy workplace environment. Workers in a safe and supportive environment feel better and are healthier, which in turn leads to decreased absenteeism, enhanced motivation, improved productivity, and promoted positive images of their enterprise.

The HEAP strategy, embodied in the prevention of occupational accidents and diseases, the promotion of a healthy work life, and building a culture of prevention, is a shared responsibility of employers and workers. The establishment of health culture requires social dialogue between workers' and employers' organizations, increased knowledge sharing, and adequate resources. In addition, social support from colleagues is an important determinant of wellbeing at work. Employees should enforce zero tolerance policies for harassment, bullying, or discrimination in the workplace.

CONCLUSION

The Healthy China 2030 Plan clearly outlines indicators and roadmaps to protect workers' health, and a series of national action plans to prevent and control occupational diseases and protect workers' health have recently been implemented, including Occupational Health Protection Campaign of Healthy China Initiative (2019–2030), Action Plan for Prevention and Control of Pneumoconiosis and HEAP (*15*). Therefore, the HEAP, consistent with international practices and the WHO's healthy workplace model, is an independent but not isolated campaign with emphasis on integrating considerable resources from governments, employers, workers, and other stakeholders to promote a healthy lifestyle and continuously improve healthy conditions for workers. It is an occupational practice shifting from a "labor approach" to a "public health approach" and is important to build a preventive public health culture in the context of the Healthy China Initiative.

doi: 10.46234/ccdcw2021.095

Corresponding author: Jun Ren, renjun@niohp.chinacdc.cn.

[1] National Institute of Occupational Health and Poison Control, Chinese Center for Disease Control and Prevention, Beijing, China.

Submitted: January 01, 2021; Accepted: January 21, 2021

REFERENCES

1. WHO. Global strategy on occupational health for all: the way to health at work. https://www.who.int/occupational_health/globstrategy/en/. [2020-9-3].
2. WHO, Burton J. WHO healthy workplace framework and model: background and supporting literature and practices. World Health Organization, 2010. https://apps.who.int/iris/handle/10665/113144. [2020-9-3].
3. WHO. Workers' health: global plan of action. https://www.who.int/occupational_health/publications/global_plan/en/. [2020-9-3].
4. WHO. Healthy workplaces: a model for action for employers, workers, policy-makers and practitioners. https://www.who.int/occupational_health/5_keys_EN_web.pdf?ua=1. [2020-9-3].
5. Iwanowicz E. The 19th meeting for the working group of the European network for workplace health promotion, July 1-2, 2005, Bratislawa, Slovakia. Med Pr 2005;56(5): 419-21. http://med.wanfangdata.com.cn/Paper/Detail/PeriodicalPaper_PM16483014.
6. Canada. The "Healthy Enterprise" Standard (BNQ9700-800). https://www.bnq.qc.ca/en/standardization/health-at-work/healthy-enterprise.html. [2020-9-3].
7. Schill AL, Chosewood LC. The NIOSH Total Worker Health^{TM} program: an overview. J Occup Environ Med 2013;55(12):S8 – 11. http://dx.doi.org/10.1097/JOM.0000000000000037.
8. David Seedhouse. TOTALHEALTH PROMOTION mental health, rational fields and the quest for autonomy. https://hshe-soh.iums.ac.ir/files/hshe-soh/files/TOTALHEALTHPROMOTION1(1).pdf. [2020-9-3].
9. Li S, Li T, Li CL, Wang C. Intervention strategies for the national project of workplace health promotion in China. Biomed Environ Sci 2015;28(5):396 – 400. http://dx.doi.org/10.3967/bes2015.056.
10. ILO. Safety and Health at the heart of the Future of Work: Building on 100 years of experience. 2019. https://www.ilo.org/tokyo/WCMS_686645/lang--en/index.htm. [2019-4-15].
11. GBD 2016 Risk Factors Collaborators. Global, regional, and national comparative risk assessment of 84 behavioural, environmental and occupational, and metabolic risks or clusters of risks, 1990–2016: a systematic analysis for the Global Burden of Disease Study 2016. Lancet 2017;390(10100):1345 – 422. http://dx.doi.org/10.1016/S0140-6736(17)32366-8.
12. China CDC. National Occupational Disease Report 2018. http://niohp.chinacdc.cn/sndt/201905/t20190531_202989.htm. [2020-9-3]. (In Chinese).
13. ILO. Working conditions in a global perspective. 2019. https://www.ilo.org/global/publications/books/WCMS_696174/lang--en/index.htm. [2019-5-6].
14. Healthy China Initiative Promotion Committee. Healthy China initiative (2019-2030). http://www.nhc.gov.cn/guihuaxxs/s3585u/201907/e9275fb95d5b4295be8308415d4cd1b2.shtml. [2020-9-3]. (In Chinese).
15. Xin Sun. Perspectives: steps forward to improve occupational health—China. China CDC Wkly 2020;2(18):310 – 3. http://dx.doi.org/10.46234/ccdcw2020.079.

Notifiable Infectious Diseases Reports

Reported Cases and Deaths of National Notifiable Infectious Diseases — China, March, 2021

Diseases	Cases	Deaths
Plague	0	0
Cholera	0	0
SARS-CoV	0	0
Acquired immune deficiency syndrome	5,951	1,710
Hepatitis	148,245	57
Hepatitis A	1,128	1
Hepatitis B	119,423	43
Hepatitis C	23,776	13
Hepatitis D	27	0
Hepatitis E	2,991	0
Other hepatitis	900	0
Poliomyelitis	0	0
Human infection with H5N1 virus	0	0
Measles	77	0
Epidemic hemorrhagic fever	424	1
Rabies	13	12
Japanese encephalitis	0	0
Dengue	0	0
Anthrax	9	0
Dysentery	3,488	0
Tuberculosis	80,803	109
Typhoid fever and paratyphoid fever	487	0
Meningococcal meningitis	7	2
Pertussis	220	0
Diphtheria	0	0
Neonatal tetanus	0	1
Scarlet fever	1,819	0
Brucellosis	7,220	1
Gonorrhea	10,878	0
Syphilis	50,682	5
Leptospirosis	7	0
Schistosomiasis	0	0
Malaria	63	0
Human infection with H7N9 virus	0	0
COVID-19*	305	0
Influenza	17,110	0
Mumps	9,604	0

Continued

Diseases	Cases	Deaths
Rubella	82	0
Acute hemorrhagic conjunctivitis	2,885	0
Leprosy	63	0
Typhus	35	0
Kala azar	13	0
Echinococcosis	430	0
Filariasis	0	0
Infectious diarrhea[†]	141,593	1
Hand, foot, and mouth disease	36,206	0
Total	**518,719**	**1,899**

[*] The data were extracted from the website of the National Health Commission of the People's Republic of China.

[†] Infectious diarrhea excludes cholera, dysentery, typhoid fever and paratyphoid fever.

The number of cases and cause-specific deaths referred to data recorded in National Notifiable Disease Reporting System (NNDRS) in China, which includes both clinically-diagnosed cases and laboratory-confirmed cases. Only reported cases of the 31 provincial-level administrative divisions in the mainland of China are included in the table, whereas data of Hong Kong Special Administrative Region, Macau Special Administrative Region, and Taiwan, China are not included. Monthly statistics were calculated without annual verification, which is usually conducted in February of the next year for de-duplication and verification of reported cases in annual statistics. Therefore, 12-month cases could not be added together directly to calculate the cumulative cases because the individual information might be verified via NNDRS according to information verification or field investigations by local CDCs.

doi: 10.46234/ccdcw2021.108

Commentary **Obituary**

Chengshi Shan (1929–2021) A Pioneer in Public Health in China

Chengshi Shan, a retired leader of the China CDC, Vice President and Communist Party of China Secretary-General of former Chinese Academy of Preventive Medicine (CAPM) (the predecessor of China CDC), passed away in Beijing on May 3, 2021 at the age of 92.

Shan was born in Huangxian City, Shandong Province (now Longkou City) in August 1929. From November 1948 to August 1949, Shan studied at Changchun Military Medical University. From August 1949 to September 1954, he served as a political faculty member at Changchun Military Medical University and Third Military Medical University, and he worked at the Chinese Academy of Medical Sciences and Peking Union Medical College afterwards. In October 1981, he served as the Secretary of the Party Committee of the Institute of Health of the Chinese Academy of Medical Sciences and, in December 1983, as the Deputy Party Secretary of the Chinese Preventive Medicine Center and later as Party Secretary of the Medical Center (Chinese Academy of Preventive Medicine) while concurrently serving as Vice President in 1988 until his retirement.

Shan had dedicated himself to preparing China for the establishment of the public health field and received special government funding to accomplish these goals. He coordinated and carefully led the design of the organizational structure of the Chinese Preventive Medicine Center (later renamed as Chinese Academy of Preventive Medicine in 1986), and he worked to establish the leadership structure for the center and its affiliate institutes.

Shan was committed to the development of graduate education and established the Health School of the Chinese Academy of Preventive Medicine and supported a group of talented individuals. He believed in and trained several of these individuals, mentored their professional careers and personal lives, actively cooperated in the department building process, and solved challenging issues in employee placement. He actively encouraged the leadership team of the academy to discuss major issues and refocus on reforms. He conducted in-depth investigations and studied at grassroots level, deepened personnel and logistics reforms, brought in new projects, guaranteed scientific and technological development, and promoted the development of the Chinese Academy of Preventive Medicine. Shan was a pioneer for China's public health field and practice and helped build several of key institutions.

Shan was principled in his methods, truth-seeking, and diligent with his responsibilities. He was hardworking, strictly self-disciplined, and easily approachable. He will be remembered dearly by his peers, students, and all those who continue his work.

Chinese Center for Disease Control and Prevention.

The inauguration of *China CDC Weekly* is in part supported by Project for Enhancing International Impact of China STM Journals Category D (PIIJ2-D-04-(2018)) of China Association for Science and Technology (CAST).

CCDC weekly

Vol. 3 No. 20 May 14, 2021

Responsible Authority

National Health Commission of the People's Republic of China

Sponsor

Chinese Center for Disease Control and Prevention

Editing and Publishing

China CDC Weekly Editorial Office

No.155 Changbai Road, Changping District, Beijing, China

Tel: 86-10-63150501, 63150701

Email: weekly@chinacdc.cn

CSSN

ISSN 2096-7071

CN 10-1629/R1